SUPPORTING INFORMATION

Probing local structure in zeolite frameworks: Ultrahigh-field NMR measurements and accurate first principles calculations of zeolite ^{29}Si magnetic shielding tensors

Darren H. Brouwer* and Gary Enright

Steacie Institute for Molecular Sciences, National Research Council

100 Sussex Drive, Ottawa ON, K1A 0R6, Canada

Email: Darren.Brouwer@nrc.ca

Complete Reference 55:

Frisch, M. J.; Trucks, G. W.; Schlegel, H. B.; Scuseria, G. E.; Robb, M. A.; Cheeseman, J. R.; Zakrzewski, V. G.; Montgomery, J. A., Jr.; Stratmann, R. E.; Burant, J. C.; Dapprich, S.; Millam, J. M.; Daniels, A. D.; Kudin, K. N.; Strain, M. C.; Farkas, O.; Tomasi, J.; Barone, V.; Cossi, M.; Cammi, R.; Mennucci, B.; Pomelli, C.; Adamo, C.; Clifford, S.; Ochterski, J.; Petersson, G. A.; Ayala, P. Y.; Cui, Q.; Morokuma, K.; Rega, N.; Salvador, P.; Dannenberg, J. J.; Malick, D. K.; Rabuck, A. D.; Raghavachari, K.; Foresman, J. B.; Cioslowski, J.; Ortiz, J. V.; Baboul, A. G.; Stefanov, B. B.; Liu, G.; Liashenko, A.; Piskorz, P.; Komaromi, I.; Gomperts, R.; Martin, R. L.; Fox, D. J.; Keith, T.; Al-Laham, M. A.; Peng, C. Y.; Nanayakkara, A.; Challacombe, M.; Gill, P. M. W.; Johnson, B.; Chen, W.; Wong, M. W.; Andres, J. L.; Gonzalez, C.; Head-Gordon, M.; Replogle, E. S.; Pople, J. A. *Gaussian 98, Revision A.11.3*, Gaussian, Inc.: Pittsburgh PA, 2002

Experimental

Pulse sequence

The recoupling pulses are timed such that the centers of the recoupling pulses were at the following fractions of the rotor period: 0.053, 0.303, 0.697, and 0.947. In odd numbered rotor periods, the indicated phases were used, while in even numbered rotor periods the phases were inverted, which leads to pulse imperfection artifacts being shifted from the center frequency to the outer edges of the CSA recoupled spectra. An eight-step phase cycle was used with the following phases for the 90° pulses: $\phi_1 = y$ or $-x$, $\phi_2 = \{y, -y\}$, $\phi_3 = \{y, y, -y, -y, -x, -x, x, x\}$, and $\phi_{rec} = \{x, -x, -x, x, y, -y, -y, y\}$. The States method was used to obtain pure adsorption lineshapes in the CSA recoupled dimension by collecting one spectrum with $\phi_1 = y$ and one with $\phi_1 = -x$ for each increment of t_1. A delay of one rotor period was used between the final two 90° pulses in order to allow spurious transverse magnetization to decay away prior to the final observe 90° pulse.

Simulations and fitting

In order to fit the CSA recoupling data, the following protocol was followed. A Fourier transformation of the direct t_2 dimension of the experimental data was first performed. The peak amplitudes in each of the spectra in t_1 were then extracted using peak positions and widths fixed to those determined from a corresponding 1D ^{29}Si MAS spectrum, giving a number of time-domain CSA recoupling curves. A series of curves were simulated under the same experimental conditions (i.e. spinning frequency and pulse lengths) for $5 \leq \Omega \leq 35$ ppm in steps of 1 ppm and $-1 \leq \kappa \leq 1$ in steps of 0.1. Each of these simulated curves was fit to the experimental data by adjusting a scaling parameter and a decay parameter to minimize the sum of the squares of the

differences, χ^2. Contour plots of χ^2 as a function of Ω and κ were constructed to locate the values of Ω and κ giving the χ^2 minimum, χ^2_{min}. The uncertainties in Ω and κ were estimated from the values of Ω and κ with $\chi^2 = 2 \times \chi^2_{min}$. The displayed experimental and best-fit simulated quasi-static CSA recoupled lineshapes were obtained by Fourier transformation of the corresponding time-domain curves and subsequent scaling of the frequency axis using the pulse sequence scaling factor of 0.393.

In order to estimate Ω and κ values and their uncertainties from the slow spinning MAS spectra, a similar protocol was applied. The spectra were first deconvoluted to give the amplitudes of the spinning sidebands for each isotropic peak. A series of spinning sideband patterns were simulated for the corresponding spinning frequency for $5 \leq \Omega \leq 35$ ppm in steps of 1 ppm and $-1 \leq \kappa \leq 1$ in steps of 0.1. Each of these simulated spinning sideband patterns was fit to the experimental amplitudes by adjusting a scaling parameter to minimize the sum of the squares of the differences, χ^2. Again, contour plots of χ^2 as a function of Ω and κ were constructed to locate the values of Ω and κ giving the minimum χ^2 and the uncertainties in Ω and κ were estimated from the values of Ω and κ with $\chi^2 = 2 \times \chi^2_{min}$. The principal components δ_{11}, δ_{22}, and δ_{33} of the CS tensor listed in Tables S1 to S3 were calculated from the determined values of δ_{iso}, Ω, and κ while their uncertainties were determined from the widest possible ranges of their values given the uncertainties in δ_{iso}, Ω, and κ. All of the fitting procedures were implemented as a *Mathematica* version 5.2 notebook.

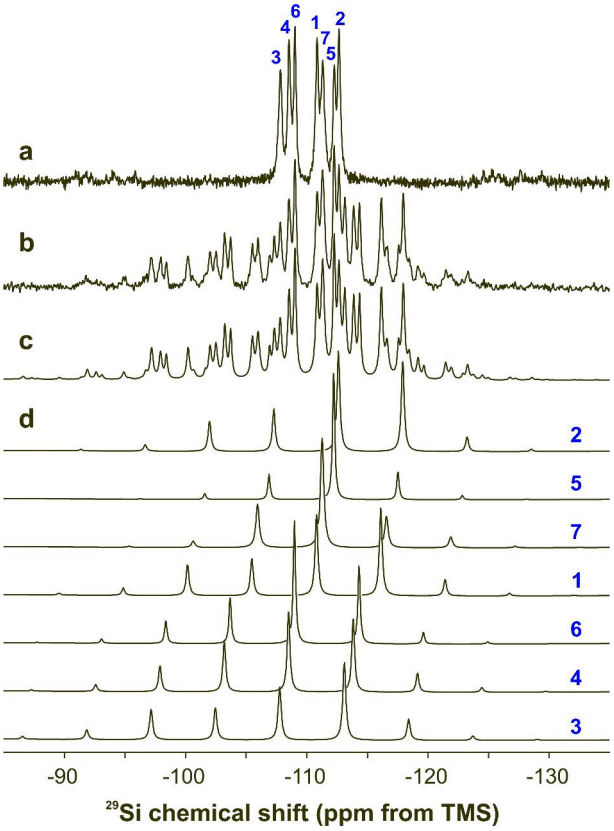

Figure S1. (a,b) Experimental ^{29}Si MAS NMR spectra of ZSM-12 obtained at MAS spinning frequencies of (a) 3000 Hz (128 scans) and (b) 950 Hz (512 scans) with recycle delays of 15 s. (c) Simulated 950 Hz MAS spectrum composed of (d) individual simulated spinning sideband patterns for each Si site. The best fit values of Ω and κ and their estimated uncertainties are listed in Table S2.

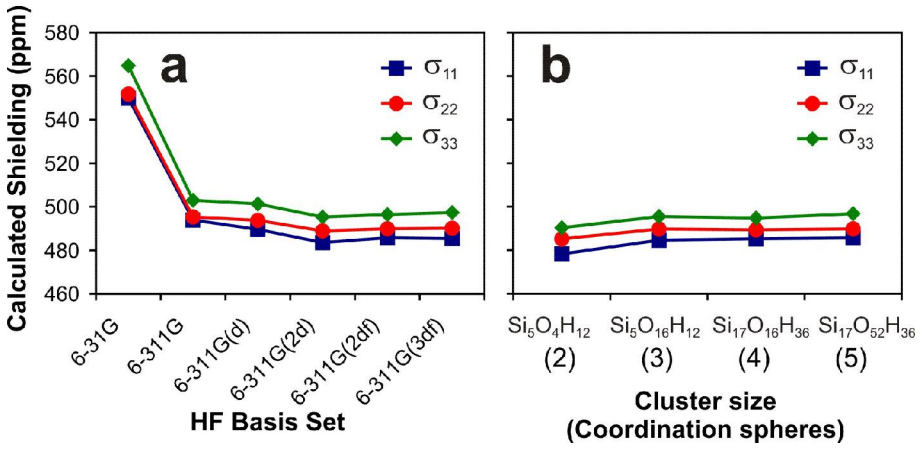

Figure S2. *Ab initio* calculated principal components of the ^{29}Si magnetic shielding tensor for the single Si site in α-quartz as functions of (d) basis set using a $Si_5O_{16}H_{12}$ cluster with three coordination spheres around the central Si atom and (e) cluster size (number of coordination spheres) around the central Si atom using the 6-311G(2df) basis set for all atoms

Table S1. Experimental and calculated principal components of the ^{29}Si chemical shift tensors for Sigma-2.

Site	δ_{iso} (ppm)	Ω (ppm)	κ	δ_{11} (ppm)	δ_{22} (ppm)	δ_{33} (ppm)
Experiment (CSA recoupling)						
Si3	-119.7 ± 0.1	8.8 ± 1.7	0.03 ± 0.25	-115.3 ± 1.4	-119.6 ± 0.9	-124.1 ± 1.4
Si1	-115.8 ± 0.1	16.4 ± 1.2	0.50 ± 0.12	-108.9 ± 1.1	-113.0 ± 1.0	-125.3 ± 1.1
Si2	-113.6 ± 0.1	18.5 ± 1.6	0.05 ± 0.18	-104.5 ± 1.5	-113.3 ± 1.2	-123.0 ± 1.5
Si4	-108.5 ± 0.1	12.6 ± 0.8	0.65 ± 0.14	-103.5 ± 0.9	-105.8 ± 0.9	-116.2 ± 0.9
Experiment (Slow MAS)						
Si3	-119.7 ± 0.1	10.7 ± 0.2	0.02 ± 0.05	-114.4 ± 0.3	-119.6 ± 0.3	-125.0 ± 0.3
Si1	-115.8 ± 0.1	17.7 ± 0.5	0.39 ± 0.06	-108.1 ± 0.5	-113.5 ± 0.5	-125.8 ± 0.5
Si2	-113.6 ± 0.1	19.3 ± 0.6	0.12 ± 0.05	-104.3 ± 0.6	-112.8 ± 0.5	-123.6 ± 0.6
Si4	-108.5 ± 0.1	14.0 ± 0.5	0.53 ± 0.13	-102.8 ± 0.7	-106.0 ± 0.8	-116.7 ± 0.7
***Ab initio* (single crystal XRD structure)**						
Si3	-119.4	9.3	0.32	-115.2	-118.4	-124.5
Si1	-115.7	16.4	0.34	-108.4	-113.8	-124.8
Si2	-113.6	21.5	-0.04	-102.7	-113.9	-124.2
Si4	-109.0	14.8	0.57	-103.0	-106.2	-117.8
***Ab initio* (powder XRD structure)**						
Si3	-119.9	8.0	0.54	-116.6	-118.4	-124.6
Si1	-116.3	25.9	0.27	-104.5	-114.0	-130.4
Si2	-112.9	21.6	0.02	-102.1	-112.7	-123.7
Si4	-109.8	17.0	0.85	-103.7	-105.0	-120.7

Table S2. Experimental and calculated principal components of the ^{29}Si chemical shift tensors for ZSM-12.

Site	δ_{iso} (ppm)	Ω (ppm)	κ	δ_{11} (ppm)	δ_{22} (ppm)	δ_{33} (ppm)
Experiment (CSA recoupling)						
Si2	-112.7 ± 0.1	21.8 ± 1.5	-0.70 ± 0.16	-99.2 ± 1.6	-117.8 ± 0.9	-121.0 ± 1.6
Si5	-112.3 ± 0.1	13.9 ± 1.9	-0.34 ± 0.21	-104.5 ± 1.6	-113.8 ± 0.8	-118.4 ± 1.6
Si7	-111.3 ± 0.1	17.6 ± 2.4	0.35 ± 0.17	-103.5 ± 1.9	-109.3 ± 1.4	-121.2 ± 1.9
Si1	-110.8 ± 0.1	23.1 ± 2.0	-0.75 ± 0.19	-96.4 ± 2.1	-116.6 ± 1.1	-119.5 ± 2.1
Si6	-109.1 ± 0.1	19.8 ± 2.4	-0.44 ± 0.21	-97.7 ± 2.2	-111.9 ± 1.1	-117.5 ± 2.2
Si4	-108.6 ± 0.1	23.5 ± 3.4	-0.26 ± 0.18	-95.8 ± 2.6	-110.6 ± 1.2	-119.3 ± 2.6
Si3	-107.8 ± 0.1	24.9 ± 3.0	-0.71 ± 0.26	-92.4 ± 3.1	-113.7 ± 1.6	-117.4 ± 3.1
Experiment (Slow MAS)						
Si2	-112.7 ± 0.1	22.8 ± 0.8	-0.65 ± 0.12	-98.8 ± 1.0	-117.6 ± 0.9	-121.6 ± 1.0
Si5	-112.3 ± 0.1	15.6 ± 0.7	-0.14 ± 0.16	-105.1 ± 0.9	-114.0 ± 0.9	-120.7 ± 0.9
Si7	-111.3 ± 0.1	18.8 ± 0.4	0.20 ± 0.07	-102.5 ± 0.5	-110.1 ± 0.6	-121.4 ± 0.5
Si1	-110.8 ± 0.1	25.0 ± 0.7	-0.61 ± 0.09	-95.8 ± 0.9	-115.9 ± 0.7	-120.8 ± 0.9
Si6	-109.1 ± 0.1	21.8 ± 0.4	-0.40 ± 0.06	-96.7 ± 0.6	-111.9 ± 0.5	-118.5 ± 0.6
Si4	-108.6 ± 0.1	26.1 ± 0.7	-0.27 ± 0.07	-94.3 ± 0.8	-110.9 ± 0.6	-120.4 ± 0.8
Si3	-107.8 ± 0.1	29.4 ± 0.6	-0.55 ± 0.05	-90.4 ± 0.7	-113.2 ± 0.5	-119.8 ± 0.7
***Ab initio* (powder XRD structure)**						
Si2	-112.7	50.5	0.09	-88.2	-111.1	-138.7
Si5	-113.4	31.5	-0.01	-97.7	-113.5	-129.2
Si7	-114.7	26.0	-0.17	-101.0	-116.2	-127.0
Si1	-108.8	28.4	-0.10	-94.1	-109.8	-122.5
Si6	-109.6	41.3	0.01	-89.0	-109.5	-130.3
Si4	-108.7	41.8	0.13	-88.7	-106.9	-130.5
Si3	-108.9	41.2	0.08	-88.8	-107.8	-130.1

Table S3. Experimental and calculated principal components of the ^{29}Si chemical shift tensors for the monoclinic phase of ZSM-5.

Site	δ_{iso} (ppm)	Ω (ppm)	κ	δ_{11} (ppm)	δ_{22} (ppm)	δ_{33} (ppm)
Experiment (CSA recoupling)						
Si8	-116.8 ± 0.1	18.8 ± 1.4	-0.25 ± 0.11	-106.6 ± 1.2	-118.3 ± 0.7	-125.4 ± 1.2
Si16	-115.8 ± 0.1	22.6 ± 1.8	-0.55 ± 0.14	-102.4 ± 1.7	-120.0 ± 0.8	-125.0 ± 1.7
Si14	-115.7 ± 0.1	22.1 ± 2.3	0.27 ± 0.16	-105.6 ± 1.9	-113.7 ± 1.5	-127.7 ± 1.9
Si11	-114.9 ± 0.1	12.9 ± 1.6	0.29 ± 0.17	-109.1 ± 1.3	-113.7 ± 1.0	-122.0 ± 1.3
Si23	-114.6 ± 0.1	17.4 ± 1.7	-0.02 ± 0.11	-105.8 ± 1.3	-114.7 ± 0.7	-123.3 ± 1.3
Si15	-114.3 ± 0.1	25.3 ± 3.0	0.32 ± 0.15	-103.0 ± 2.4	-111.7 ± 1.7	-128.3 ± 2.4
Si17	-114.1 ± 0.1	20.6 ± 3.0	0.15 ± 0.17	-104.3 ± 2.3	-113.1 ± 1.4	-124.9 ± 2.3
Si6	-113.9 ± 0.1	23.3 ± 2.5	0.26 ± 0.14	-103.2 ± 2.0	-111.9 ± 1.4	-126.6 ± 2.0
Si19	-113.4 ± 0.1	14.8 ± 1.1	-0.62 ± 0.14	-104.4 ± 1.1	-116.4 ± 0.6	-119.2 ± 1.1
Si9	-112.6 ± 0.1	22.3 ± 1.9	-0.02 ± 0.12	-101.4 ± 1.5	-112.7 ± 1.0	-123.7 ± 1.5
Si13	-112.5 ± 0.1	24.7 ± 2.6	-0.52 ± 0.16	-98.0 ± 2.3	-116.8 ± 0.9	-122.7 ± 2.3
Si22	-112.3 ± 0.1	19.1 ± 1.9	0.33 ± 0.13	-103.8 ± 1.6	-110.2 ± 1.2	-122.9 ± 1.6
Si10	-111.8 ± 0.1	18.7 ± 2.3	0.34 ± 0.19	-103.6 ± 2.0	-109.7 ± 1.5	-122.2 ± 2.0
Si5	-111.5 ± 0.1	22.6 ± 3.2	0.10 ± 0.18	-100.6 ± 2.4	-110.8 ± 1.6	-123.2 ± 2.4
Si21	-109.6 ± 0.1	25.4 ± 3.6	0.04 ± 0.15	-97.0 ± 2.6	-109.3 ± 1.4	-122.5 ± 2.6
Si3	-113.7 ± 0.2	-	-	-	-	-
Si4	-113.7 ± 0.2	-	-	-	-	-
Si12	-113.7 ± 0.2	-	-	-	-	-
Si18	-113.7 ± 0.2	-	-	-	-	-
Si24	-113.7 ± 0.2	-	-	-	-	-
Si1	-113.1 ± 0.2	-	-	-	-	-
Si2	-113.1 ± 0.2	-	-	-	-	-
Si7	-113.1 ± 0.2	-	-	-	-	-
Si20	-113.1 ± 0.2	-	-	-	-	-
Ab initio **(single crystal XRD structure)**						
Si8	-117.0	14.0	-0.25	-109.4	-118.1	-123.4
Si16	-116.3	15.3	-0.36	-107.7	-118.1	-123.0
Si14	-116.1	17.1	0.01	-107.6	-116.0	-124.7
Si11	-115.1	9.9	0.19	-110.4	-114.4	-120.3
Si23	-115.0	12.6	-0.02	-108.6	-115.0	-121.3
Si15	-114.8	17.0	0.29	-107.2	-113.2	-124.2
Si17	-114.3	17.3	0.06	-105.8	-113.9	-123.1
Si6	-114.9	19.0	0.10	-105.7	-114.3	-124.7
Si19	-114.0	10.7	-0.40	-107.9	-115.4	-118.6
Si9	-112.8	20.0	-0.08	-102.6	-113.4	-122.5
Si13	-113.2	22.3	-0.44	-100.4	-116.4	-122.7
Si22	-112.4	18.6	0.02	-103.2	-112.3	-121.8
Si10	-112.2	18.4	0.03	-103.1	-111.9	-121.4
Si5	-112.0	18.0	-0.08	-102.8	-112.5	-120.8
Si21	-110.1	20.8	-0.01	-99.6	-110.1	-120.4
Si3	-114.0	16.5	-0.12	-105.5	-114.7	-121.9
Si4	-113.8	14.9	0.07	-106.6	-113.5	-121.5
Si12	-113.9	21.0	-0.34	-102.1	-116.2	-123.2
Si18	-114.2	18.0	0.28	-106.0	-112.5	-124.0
Si24	-113.8	14.8	-0.26	-105.8	-115.1	-120.5
Si1	-113.9	23.6	-0.53	-100.0	-118.1	-123.7
Si2	-113.5	19.9	0.27	-104.5	-111.7	-124.3
Si7	-113.7	10.4	0.10	-108.6	-113.3	-119.1
Si20	-113.8	17.0	0.13	-105.7	-113.1	-122.7

Table S4. Crystal data and structure refinement for Sigma-2.

Identification code	db10_0m	
Empirical formula	C40 H60 N4 O128 Si64	
Formula weight	4442.68	
Temperature	296(2) K	
Wavelength	0.71073 Å	
Crystal system	Tetragonal	
Space group	I41/amd	
Unit cell dimensions	a = 10.23160(10) Å	α= 90°.
	b = 10.23160(10) Å	β= 90°.
	c = 34.3642(6) Å	γ = 90°.
Volume	3597.44(8) $Å^3$	
Z	1	
Density (calculated)	2.051 Mg/m^3	
Absorption coefficient	0.683 mm^{-1}	
F(000)	2248	
Crystal size	0.10 x 0.10 x 0.08 mm^3	
Theta range for data collection	2.08 to 40.22°.	
Index ranges	-18<=h<=16, -18<=k<=15, -62<=l<=62	
Reflections collected	37855	
Independent reflections	3045 [R(int) = 0.0422]	
Completeness to theta = 40.22°	99.4 %	
Absorption correction	Semi-empirical from equivalents	
Max. and min. transmission	0.9474 and 0.9348	
Refinement method	Full-matrix least-squares on F^2	
Data / restraints / parameters	3045 / 178 / 166	
Goodness-of-fit on F^2	1.047	
Final R indices [I>2sigma(I)]	R1 = 0.0271, wR2 = 0.0703	
R indices (all data)	R1 = 0.0346, wR2 = 0.0740	
Largest diff. peak and hole	0.528 and -0.432 $e.Å^{-3}$	

Table S5. Atomic coordinates (x 10^4) and equivalent isotropic displacement parameters ($Å^2$x 10^3) for Sigma-2. U(eq) is defined as one third of the trace of the orthogonalized U^{ij} tensor.

	x	y	z	U(eq)
Si(1)	2857(1)	2500	1183(1)	9(1)
Si(2)	2817(1)	5000	0	11(1)
Si(3)	1534(1)	2500	347(1)	9(1)
Si(4)	1510(1)	2500	1955(1)	10(1)
O(1)	0	2500	2067(1)	27(1)
O(2)	2193(1)	1220(1)	2130(1)	26(1)
O(3)	2285(1)	2500	753(1)	19(1)
O(4)	1675(1)	2500	1491(1)	16(1)
O(5)	0	2500	423(1)	22(1)
O(6)	1913(1)	3774(1)	101(1)	21(1)
O(7)	3721(1)	3779(1)	1250	26(1)
N(1)	336(11)	5150(12)	871(3)	92(3)
C(1)	157(10)	6372(9)	1069(3)	85(2)
C(2)	-1249(10)	6835(10)	1018(4)	87(2)
C(3)	1060(11)	7388(9)	881(3)	84(2)
C(4)	456(14)	6163(10)	1501(3)	85(2)
C(5)	-1403(10)	8157(10)	1231(3)	88(2)
C(6)	971(11)	8687(10)	1106(3)	83(2)
C(7)	324(9)	7475(11)	1710(3)	86(2)
C(8)	-439(10)	9166(11)	1073(4)	86(2)
C(9)	1284(13)	8453(14)	1531(3)	85(2)
C(10)	-1070(11)	7950(15)	1658(3)	87(2)

*Note that the Si and O uncertainties have been rounded. See the cif file for the actual uncertainties.

Table S6. Bond lengths [Å] and angles [°] for Sigma-2 framework.

Si(1)-O(3)	1.5887(7)	O(7)#1-Si(1)-O(4)	108.70(3)
Si(1)-O(7)	1.5961(3)	O(6)#2-Si(2)-O(6)	109.21(5)
Si(1)-O(7)#1	1.5961(3)	O(6)#2-Si(2)-O(2)#3	110.61(4)
Si(1)-O(4)	1.6078(7)	O(6)-Si(2)-O(2)#3	108.45(3)
Si(2)-O(6)#2	1.5956(6)	O(6)#2-Si(2)-O(2)#4	108.45(3)
Si(2)-O(6)	1.5956(6)	O(6)-Si(2)-O(2)#4	110.61(4)
Si(2)-O(2)#3	1.6020(6)	O(2)#3-Si(2)-O(2)#4	109.51(5)
Si(2)-O(2)#4	1.6020(6)	O(5)-Si(3)-O(3)	109.27(6)
Si(3)-O(5)	1.5914(3)	O(5)-Si(3)-O(6)	109.07(4)
Si(3)-O(3)	1.5938(7)	O(3)-Si(3)-O(6)	110.19(3)
Si(3)-O(6)	1.6015(6)	O(5)-Si(3)-O(6)#5	109.07(4)
Si(3)-O(6)#5	1.6015(6)	O(3)-Si(3)-O(6)#5	110.19(3)
Si(4)-O(1)	1.5926(4)	O(6)-Si(3)-O(6)#5	109.03(5)
Si(4)-O(2)#5	1.6018(6)	O(1)-Si(4)-O(2)#5	109.40(3)
Si(4)-O(2)	1.6018(6)	O(1)-Si(4)-O(2)	109.40(3)
Si(4)-O(4)	1.6041(7)	O(2)#5-Si(4)-O(2)	109.69(6)
O(1)-Si(4)#6	1.5926(4)	O(1)-Si(4)-O(4)	110.02(5)
O(2)-Si(2)#1	1.6020(6)	O(2)#5-Si(4)-O(4)	109.17(3)
O(5)-Si(3)#6	1.5914(3)	O(2)-Si(4)-O(4)	109.17(3)
O(7)-Si(1)#3	1.5961(3)	Si(4)#6-O(1)-Si(4)	152.03(8)
		Si(4)-O(2)-Si(2)#1	148.82(5)
O(3)-Si(1)-O(7)	109.81(2)	Si(1)-O(3)-Si(3)	172.80(6)
O(3)-Si(1)-O(7)#1	109.81(2)	Si(4)-O(4)-Si(1)	137.25(5)
O(7)-Si(1)-O(7)#1	110.20(8)	Si(3)#6-O(5)-Si(3)	160.88(9)
O(3)-Si(1)-O(4)	109.59(4)	Si(2)-O(6)-Si(3)	153.47(4)
O(7)-Si(1)-O(4)	108.70(3)	Si(1)#3-O(7)-Si(1)	158.25(8)

Symmetry transformations used to generate equivalent atoms:

#1 -y+3/4,x-1/4,-z+1/4 #2 x,-y+1,-z #3 y+1/4,-x+3/4,-z+1/4

#4 y+1/4,x+1/4,z-1/4 #5 x,-y+1/2,z #6 -x+0,-y+1/2,z+0

Table S7. Anisotropic displacement parameters ($Å^2 x\ 10^3$) for Sigma-2. The anisotropic displacement factor exponent takes the form: $-2\pi^2[\ h^2 a^{*2} U^{11} + ... + 2\ h\ k\ a^*\ b^*\ U^{12}\ ]$

	U^{11}	U^{22}	U^{33}	U^{23}	U^{13}	U^{12}
Si(1)	8(1)	11(1)	8(1)	0	-1(1)	0
Si(2)	11(1)	10(1)	11(1)	2(1)	0	0
Si(3)	8(1)	9(1)	9(1)	0	-1(1)	0
Si(4)	8(1)	14(1)	8(1)	0	0(1)	0
O(1)	8(1)	60(1)	14(1)	0	0	0
O(2)	35(1)	25(1)	20(1)	9(1)	4(1)	13(1)
O(3)	19(1)	30(1)	9(1)	0	-4(1)	0
O(4)	13(1)	25(1)	9(1)	0	2(1)	0
O(5)	8(1)	29(1)	29(1)	0	0	0
O(6)	25(1)	16(1)	22(1)	8(1)	-6(1)	-9(1)
O(7)	25(1)	25(1)	29(1)	-3(1)	-3(1)	-15(1)
N(1)	92(4)	88(4)	96(4)	-6(3)	0(3)	-1(3)
C(1)	86(3)	83(2)	85(2)	-4(2)	2(2)	0(2)
C(2)	84(3)	89(3)	88(3)	-4(3)	-2(3)	-1(3)
C(3)	85(3)	84(3)	83(3)	-1(3)	10(3)	0(3)
C(4)	88(3)	84(3)	85(3)	2(3)	1(3)	2(3)
C(5)	85(3)	91(3)	86(3)	-1(2)	0(3)	4(3)
C(6)	85(3)	82(3)	83(3)	1(3)	5(2)	0(2)
C(7)	87(3)	90(3)	81(3)	1(3)	-4(2)	1(3)
C(8)	87(3)	86(3)	84(3)	2(3)	2(3)	1(3)
C(9)	86(3)	86(3)	84(3)	1(3)	-2(3)	0(3)
C(10)	87(3)	91(3)	83(3)	1(3)	0(3)	3(3)

Table S8. Hydrogen coordinates (x 10^4) and isotropic displacement parameters ($Å^2$x 10^3) for Sigma-2.

	x	y	z	U(eq)
H(2A)	-1848	6197	1126	104
H(2B)	-1447	6939	743	104
H(3A)	805	7525	612	101
H(3B)	1953	7073	884	101
H(4A)	-151	5535	1611	103
H(4B)	1336	5826	1532	103
H(5)	-2301	8478	1204	105
H(6)	1573	9332	995	100
H(7)	515	7364	1988	103
H(8A)	-534	9975	1218	103
H(8B)	-640	9346	803	103
H(9A)	1236	9274	1672	102
H(9B)	2168	8119	1555	102
H(10A)	-1184	8766	1798	105
H(10B)	-1666	7314	1769	105